COMPARISON OF VARIOUS SOURCES OF COHERENT THz RADIATION AT FLUTE

M. Schwarz*, E. Huttel, A. S. Müller, S. Naknaimueang, M. J. Nasse, R. Rossmanith, M. Schuh, P. Wesolowski, Karlsruhe Institute of Technology, Germany
M. Schmelling, Max-Planck Institute for Nuclear Physics, Heidelberg, Germany

Abstract

The "Ferninfrarot Linac- Und Test-Experiment" FLUTE, based on a 50 MeV S-band linac with bunch compressor, is funded by –and in the final design phase at– the KIT in Karlsruhe in order to study the production of coherent radiation in the Terahertz frequency range. The three photon generating mechanisms investigated in this paper are coherent synchrotron-, edge-, and transition radiation. For each case, we present the spectra calculated from longitudinal charge distributions of a short, low charge and a long, high charge bunch. The respective bunch shapes are obtained by a detailed simulation (particle tracking) of FLUTE. We also give the expected electric field pulses.

INTRODUCTION

The purpose of FLUTE is to investigate the production of coherent THz radiation. Funded by KIT, it consists of a 7 MeV rf-gun, a 50 MeV linac, and a four magnet chicane. For details consult [1, 2]. In this paper, we compute the spectra and electric field pulses for a short, low charge and a long, high charge bunch obtained by detailed particle tracking [2]. Spectra are obtained for coherent synchrotron-, edge-, and transition radiation, while the pulses are calculated for the synchrotron radiation only.

INTENSITIES

An electric charge emits electromagnetic radiation if it is either accelerated or passes a boundary between two media. The former case includes synchrotron- and edge radiation in a dipole magnet, while transition radiation is an examples of the latter. Independently of the exact generation mechanism, an observer at distance R form the source receives a spectral intensity I radiated into the solid angle $\mathrm{d}\Omega$ given by [3]

$$\frac{\mathrm{d}^2 I}{\mathrm{d}\omega \mathrm{d}\Omega} = 2\epsilon_0\, c\, R^2 \left|\boldsymbol{E}(\omega)\right|^2 , \tag{1}$$

where $E(\omega)$ is the Fourier transformed electric field

$$\boldsymbol{E}(\omega) \equiv \frac{1}{\sqrt{2\pi}} \int_{-\infty}^{\infty} \boldsymbol{E}(t) \mathrm{e}^{\mathrm{i}\omega\, t} \mathrm{d}t\,.$$

We use SI units throughout the paper, and c, ϵ_0, and e denote the speed of light, vacuum permittivity and the electron charge, respectively. Furthermore, γ is the Lorentz factor and $\beta \equiv v/c$ is the electron speed. The coordinate system is the one conventionally used in accelerator physics. Namely, z is the direction of the momentary particle velocity, while x and y are the horizontal and vertical directions, respectively.

The total electric field of a particle bunch is obtained by summing the fields of each particle, taking into account phase differences. Using this total field in equation (1) then gives the radiated intensity of a bunch. The result reads

$$\left.\frac{\mathrm{d}^2 I}{\mathrm{d}\omega \mathrm{d}\Omega}\right|_{\text{bunch}} = N \left[1 + (N-1)\, F(\omega)\right] \left.\frac{\mathrm{d}^2 I}{\mathrm{d}\omega \mathrm{d}\Omega}\right|_{\text{single}} . \tag{2}$$

Here, N denotes the number of electrons in the bunch and $\mathrm{d}^2 I/\mathrm{d}\omega\mathrm{d}\Omega|_{\text{single}}$ is the spectral intensity of a single electron. The form factor $F(\omega)$ of the normalized charge distribution $\rho(\boldsymbol{x})$ is defined by

$$F(\omega) \equiv \left| \int \rho(\boldsymbol{x})\, \mathrm{e}^{\mathrm{i}\omega \hat{\boldsymbol{n}}\cdot \boldsymbol{r}/c} \mathrm{d}^3 x \right|^2 . \tag{3}$$

While the integration is over all of space, it is sufficient for our applications to focus on the longitudinal direction.

As can be seen in equation (2), the spectral power naturally splits into an incoherent and coherent part. The interest in the latter comes from the fact that it is enhanced over the incoherent part by a factor of N, which can easily be of the order of 10^8. On the other hand, however, the form factor drops exponentially for wavelengths smaller than the bunch length. Producing coherent THz radiation thus requires bunches shorter than a picosecond.

Synchrotron radiation (SR) occurs when an electron moves in the field of a dipole magnet on a circle of radius ϱ. The spectral intensity for a single electron then equals [3]

$$\left.\frac{\mathrm{d}^2 I}{\mathrm{d}\omega \mathrm{d}\Omega}\right|_{\text{SR}} = \frac{e^2\, \omega^2\, \varrho^2}{12\pi^3 \epsilon_0\, c^3} \left(\frac{1+\gamma^2\vartheta^2}{\gamma^2}\right)^2 \left\{ K^2_{2/3}[\xi(\omega,\vartheta)] + \frac{\gamma^2\vartheta^2}{1+\gamma^2\theta^2} K^2_{1/3}[\xi(\omega,\vartheta)] \right\} . \tag{4}$$

Here, K_q denote the modified Bessel functions and

$$\xi(\omega,\vartheta) \equiv \frac{\omega}{2\omega_{\mathrm{c}}} \left(1+\gamma^2\vartheta^2\right)^{3/2} ,$$

with the critical frequency $\omega_{\mathrm{c}} \equiv 3\gamma^3\, c/2\rho$. Expressed in standard spherical polar coordinates (θ,ϕ) the angle ϑ used in equation (4) by [3] is given by $\tan\vartheta = \sin\theta \sin\phi / \sqrt{1-\sin^2\theta^2 \sin\phi}$.

* markus.schwarz@kit.edu

ISBN 978-3-95450-115-1

Edge radiation (ER) occurs as the electron enters or exits a bending magnet. In the zero edge length model the spectral intensity reads [4]

$$\left.\frac{\mathrm{d}^2 I}{\mathrm{d}\omega \mathrm{d}\Omega}\right|_{\mathrm{ER}} = \frac{e^2}{2\,(2\pi)^3\,\epsilon_0\,c}\,\frac{\beta^2 \sin^2\theta}{(1-\beta\cos\theta)^2}\,. \tag{5}$$

Since the model assumes that the acceleration occurs not over a finite distance d but instantaneously, equation (5) is independent of frequency. Furthermore, the validity of equation (5) is limited by $\gamma^2\,c/100L < \nu < \gamma^2\,c/d$ [4]. We take the straight section length L to be the length of a bending magnet.

The backward transition radiation (TR) emitted by an electron hitting a disc of radius a is given by [5]

$$\left.\frac{\mathrm{d}^2 I}{\mathrm{d}\omega \mathrm{d}\Omega}\right|_{\mathrm{TR}} = \frac{2e^2}{(2\pi)^3\,\epsilon_0 c}\,\frac{\beta^2 \sin^2\theta}{(1-\beta^2\cos^2\theta)^2}\left[1 - T(\omega\,a,\theta)\right]^2, \tag{6}$$

with

$$T(\omega\,a,\theta) \equiv \frac{\omega\,a}{c\,\beta\,\gamma} J_0\left(\frac{\omega\,a\sin\theta}{c}\right) K_1\left(\frac{\omega\,a}{c\,\beta\gamma}\right) + \frac{\omega\,a}{c\beta^2\gamma^2\sin\theta} J_1\left(\frac{\omega\,a\sin\theta}{c}\right) K_0\left(\frac{\omega\,a}{c\,\beta\gamma}\right),$$

and J_n denoting the Bessel functions.

SPECTRA

To calculate the coherent spectra, we use a 0.1 nC and 3 nC bunch obtained by detailed simulation of FLUTE [2]. Longitudinal profiles are shown in Fig. 1. The profile of the 0.1 nC was approximated by three straight line sections, while the 3 nC bunch is a Gaussian with $\sigma \simeq 417$ fs. These approximations were used to calculate the form factors analytically. Bending radii of the chicane magnets were 3.9 m and 3.4 m for the 0.1 nC and 3 nC bunch, respectively. Both bunches had a mean energy of 41 MeV.

The detector with an aperture $\theta_{\mathrm{max}} = 0.2$ rad is assumed to be at a distance $R = 1$ m from the source. Integrating equations (4)–(6) over $\mathrm{d}\Omega$ then yields the spectra shown in Fig. 2. Assuming typical parameters for FLUTE ($L \simeq 0.5$ m, $d \simeq \rho/\gamma$, $\rho \simeq 3.5$ m) shows that the range of validity of the zero edge length model for CER equals 4×10^{-2} THz $< \nu \ll 40$ THz and corresponds to our frequency range of interest.

Notice that CSR yields the largest spectrum for both bunches. For small frequencies, the form factor approaches 1 and the spectra of the 3 nC bunch are larger by a factor of $N^2_{3\,\mathrm{nC}}/N^2_{0.1\,\mathrm{nC}} \simeq 900$. At frequencies above 1 THz, however, the Gaussian form factor of the 3 nC leads to an exponential suppression of coherent radiation. Because the 0.1 nC bunch is non-Gaussian and shorter overall, its spectra extend to higher frequencies and do not drop as rapidly. Therefore, the 0.1 nC bunch is better suited for applications that require THz radiation.

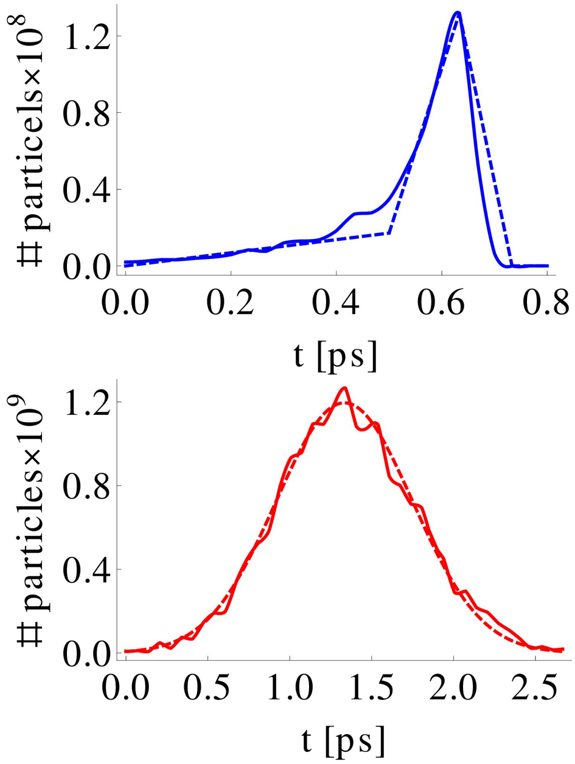

Figure 1: Longitudinal charge profile for bunches with total charge of 0.1 nC (top) and 3 nC (bottom). Dashed curves are approximations with the same total charge.

ELECTRIC PULSE

We calculate the electric pulse of an SR emitting bunch following [6]. The radiated electric field of a single electron is assumed to be a solution of a one-dimensional wave equation with amplitude $E_0(\omega)$ and phase ϕ. Summing the fields of all electrons in the bunch yields

$$\frac{E(t)}{N} = \mathrm{Re}\left[\mathrm{e}^{-\mathrm{i}\phi}\int_0^\infty E_0(\omega)\int_{-\infty}^{\infty} \mathrm{e}^{\mathrm{i}\omega(z/c-t)}\rho(z)\mathrm{d}z\mathrm{d}\omega\right]. \tag{7}$$

For the amplitude $E_0(\omega)$ we take

$$E_0(\omega) \equiv \sqrt{\int |\boldsymbol{E}(\omega)|^2 \mathrm{d}\Omega} = \sqrt{\int \frac{1}{2\epsilon_0\,c}\frac{\mathrm{d}I}{\mathrm{d}\omega\mathrm{d}\Omega}}$$
$$\simeq \frac{e\sqrt{\gamma}}{\sqrt{4\pi}\epsilon_0\,c\,R}\,\frac{27^{1/4}}{4^{1/3}}\,\sqrt{\Gamma(5/3)}\left(\frac{\omega}{\omega_c}\right)^{1/6}. \tag{8}$$

The last line is the low frequency approximation to the $\mathrm{d}\Omega$ integral of the SR spectrum given in equation (4) [3]. This approximation, together with the approximations of $\rho(z)$ mentioned in the last section, allows us to solve equation (7) analytically. Because the integration in equation (8) is over the full solid angle, we do not take focusing into account. However, most of the SR is emitted inside a cone with opening angle $1/\gamma$. At a distance of $R = 1$ m this gives a spot radius of about 12 mm. Assuming a focusing down to a spot radius of 1 mm would then yield a factor 144 in field strength.

ISBN 978-3-95450-115-1

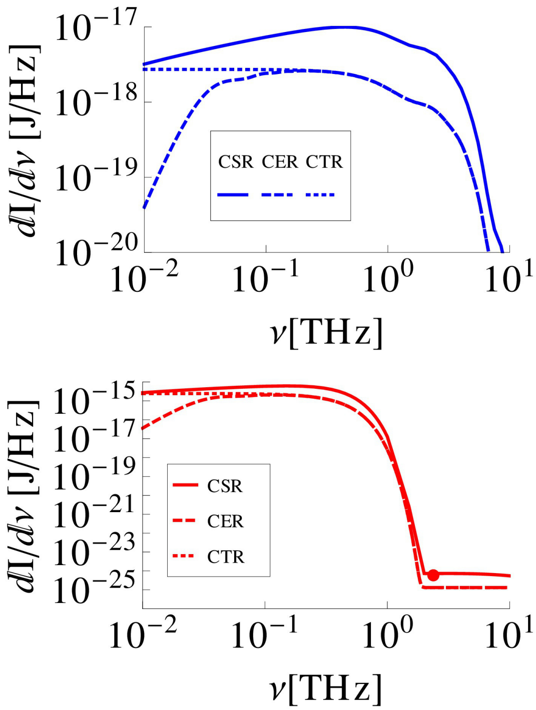

Figure 2: Spectra for the 0.1 nC (top) and 3 nC (bottom) bunch. The dot at 2.4 THz marks the SR spectrum at the frequency corresponding to σ.

For the 0.1 nC bunch, we solve equation (7) analytically by using Fourier sine and cosine transformations. We refrain from giving the lengthy expression, but refer to Fig. 3 for the result, instead.

Using a Gaussian profile for the 3 nC bunch, the integration in equation (7) can again be performed analytically. The final result reads

$$E(\tau) = \frac{e\sqrt{\gamma\Gamma(5/3)}}{\sqrt{4\pi\epsilon_0}\,c\,R}\,\frac{27^{1/4}}{2\,2^{1/12}}\,\frac{N}{(\sigma^7\omega_c/c^7)^{1/6}} \times\Bigg[\Gamma(\frac{7}{12})\,{}_1F_1\left(\frac{7}{12},\frac{1}{2},\frac{-\tau^2}{2}\right)\cos\phi - \sqrt{2}\Gamma(\frac{13}{12})\,\tau\,{}_1F_1\left(\frac{13}{12},\frac{3}{2},\frac{-\tau^2}{2}\right)\sin\phi\Bigg], \quad (9)$$

where ${}_1F_1$ is Kummer's confluent hypergeometric function [7] and $\tau \equiv t\,c/\sigma$. The pulse for $\phi = 325°$ is shown in Fig. 3.

Both pulses show the "single cycle" shape for $\phi = 325°$. To create pulse lengths of the order of picoseconds requires significant spectral power in the THz regime. As can be seen in Fig. 2, the spectrum of the 3 nC bunch is smaller by several orders of magnitude in the THz regime, compared to that of the 0.1 nC bunch. As a result, the peak electric field is larger by only a factor of three even though the bunch charge is larger by a factor of 30.

CONCLUSION

Using the profiles of a short, low charge and a long, high charge electron bunch obtained by detailed particle tracking of FLUTE [2], we computed the spectra for CSR, CER, and CTR. Since a coherent spectrum is independent of the bunch form for low frequencies, the spectra of the high charge bunch are larger in this frequency regime. However, the situation reverses for frequencies above 1 THz, where the Gaussian form factor of the high charge bunch leads to an exponential suppression. This lack of spectral power is also the reason why the peak electric field of the long bunch is only three times higher than that of the low charge one.

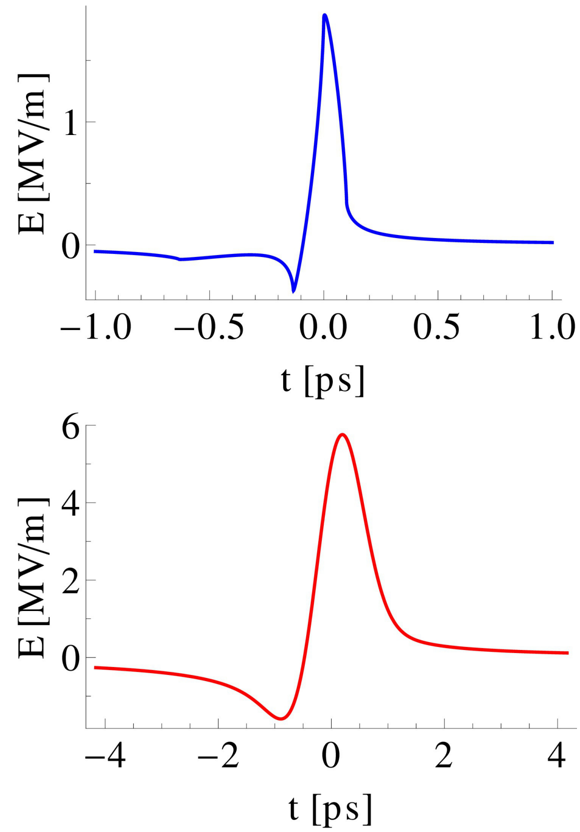

Figure 3: Unfocused THz-pulses at a distance of 1m from the source, emitted by the 0.1 nC (top) and 3 nC bunch (bottom), respectively. In both cases $\phi = 325°$.

REFERENCES

[1] S. Naknaimueang et al., TUPO007, IPAC 2011 (2011).

[2] S. Naknaimueang et al., TUPPP012, IPAC 2012 (2012).

[3] J. Jackson, Classical Electrodynamics, John Wiley&Sons, 3rd ed., 1999.

[4] R.A. Bosch, Nouv. Cim. **20**, 483 (1998).

[5] S. Casalbuoni et al., Phys. Rev. ST Accel. Beams **8**, 030705 (2009).

[6] A.-S. Müller, RAST **3**, 165 (2010).

[7] I.S. Gradshteyn and I.M. Ryzhik, Table of Integrals, Series, and Products, Elsevier, 7th ed., 2007.